



THERMAL ANALYSIS IN SUPPORT OF THE BOOSTER SEPARATION MOTOR CRACK INVESTIGATION

Darrell Davis
NASA/MSFC/ED25

Thermodynamics and Heat Transfer Group

Terry Prickett
NASA/MSFC/ED25

Thermodynamics and Heat Transfer Group

ABSTRACT

During a post-test inspection of a Booster Separation Motor (BSM) from a Lot Acceptance Test (LAT), a crack was noticed in the graphite throat. Since this was an out-of-family occurrence, an investigation team was formed to determine the cause of the crack. This paper will describe thermal analysis techniques used in support of this investigation. Models were generated to predict gradients in nominal motor conditions, as well as potentially anomalous conditions. Analysis was also performed on throats that were tested in the Laser Hardened Material Evaluation Laboratory (LHMEL). Some of these throats were pre-cracked, while others represented configurations designed to amplify effects of thermal stresses. Results from these analyses will be presented in this paper.

INTRODUCTION

Booster Separation Motors (BSM) are small solid propellant motors attached to the Frustum and Aft Skirt of the Solid Rocket Boosters (SRB). These motors have a throat diameter of 3.13 inches and fire for approximately 0.8 seconds. The purpose of the motors is to provide a thrust vector to the SRBs at separation to guide them away from possible contact with the orbiter.

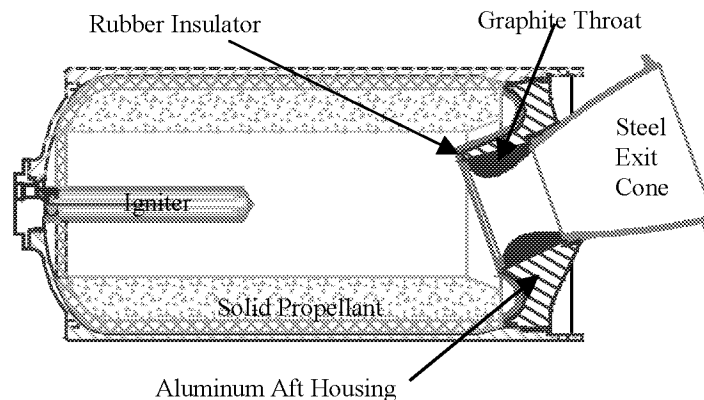


Figure 1: BSM Cross Section

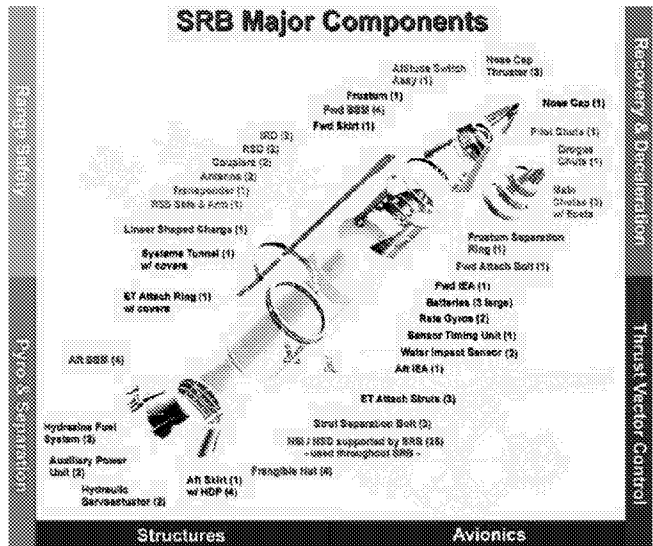


Figure 2: SRB Components Showing Location of BSMs

These motors are manufactured by Pratt & Whitney's Chemical Science's Division (CSD) near San Jose, California. A lot of BSMs consist of 160 motors manufactured with similar characteristics. From each lot, two motors are chosen for Lot Acceptance Tests (LAT). The motors are preconditioned hot and cold, 120F and 30F, and fired. The purchase of the lots is dependent on the results of the LAT. Testing of the lot designated ABM was performed in December 2000. Since it was near the Christmas holiday, the two BSMs were packed into crates and left under an overhang. In early January, the motors were removed and subjected to the post-test inspection. At that time it was noticed that the forward end of the graphite throat had a crack.



Figure 3: Crack in Graphite Throat

During the history of the BSM program, a crack had never been detected in a BSM throat. Since this was an out-of-family occurrence, an anomaly investigation team was formed. (Further investigation revealed that this might not have been as rare as was thought. Even though eight BSMs fly on each SRB, 16 per flight, very few had been subjected to the type of inspection that would have seen such a crack. Most of the throats on the aft BSMs are shoved into the BSM case at splashdown and are damaged beyond the point of reasonable inspection. The typical inspection routine for the forward BSMs was a simple visual inspection to ensure there was no catastrophic failure or out-of-family erosion of the throat. BSMs from the first three shuttle flights, the first two post-Challenger flights and every one of the LAT BSMs were inspected in-depth.)

MODEL DESCRIPTION

The Thermodynamics and Heat Transfer Group was tasked to generate thermal profiles to be used as an input to stress models. Although the throat is symmetric and could be modeled with a 2-D model, the aft housing is not symmetric and provides a non-uniform heat sink. Therefore it was decided to create a 3-D SINDA model. PATRAN was used for pre- and post-processing of the SINDA model. Figure 4 shows the elemental composition of the model as well as a graphic illustrating the locations of the different materials.

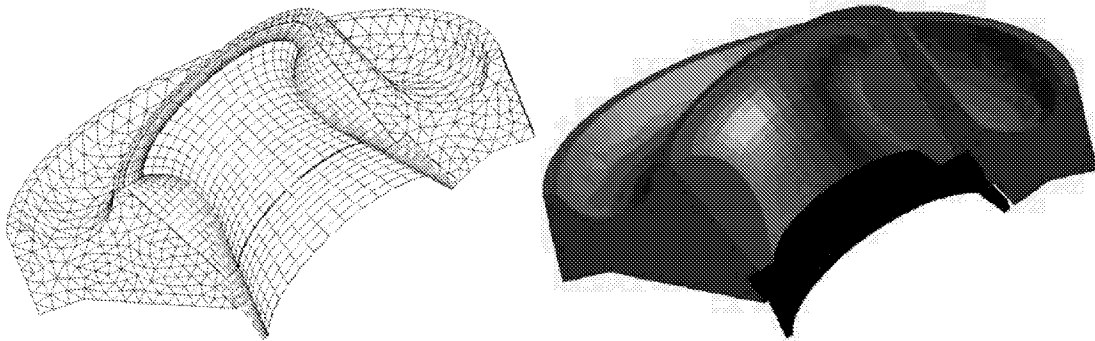


Figure 4: PATRAN Pre-processing Graphics

Boundary conditions and material properties were provided by CSD. The Aerothermal Chemical Equilibrium (ACE) code was used to calculate combustion gas properties within the chamber. UARLED was used to calculate gas static and recovery temperatures as well as boundary layer temperatures and heat transfer coefficients (HTCs). The HTCs were adjusted by empirical constants based on CSD's experience with actual measured responses from many similar programs. These boundary conditions have been used by CSD since the inception of the BSM program. Figure 5 shows recovery temperature as a function of axial location. The analysis assumed no circumferential variation in temperature at a specific location. Figure 6 shows a multiplying factor applied to the recovery temperature to account for the effect of Propellant Mean Bulk Temperature (PMBT) on the ballistics of the motor. Therefore the recovery temperatures used in the analysis to predict surface temperatures were functions of time and location. Figure 7 illustrates the values of the heat transfer coefficients as a function of time.

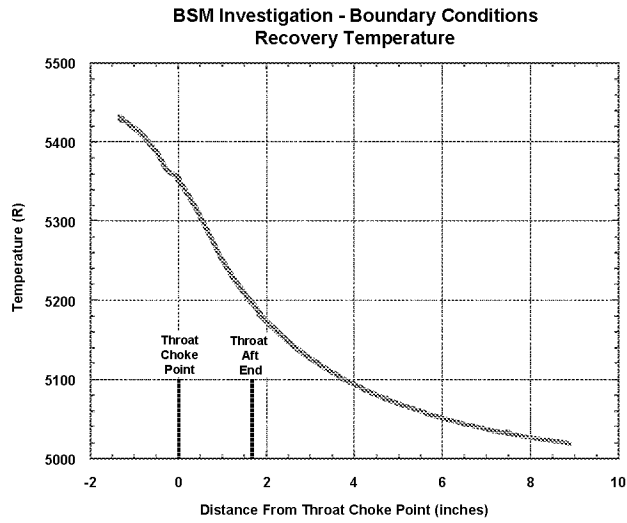


Figure 5: Recovery Temperature

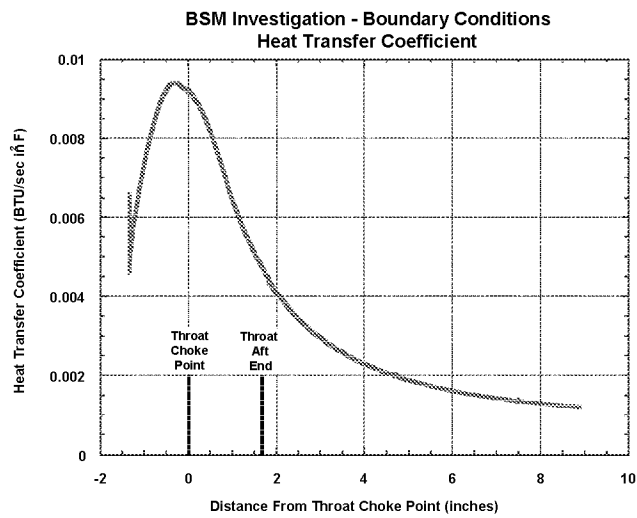


Figure 6: Heat Transfer Coefficient

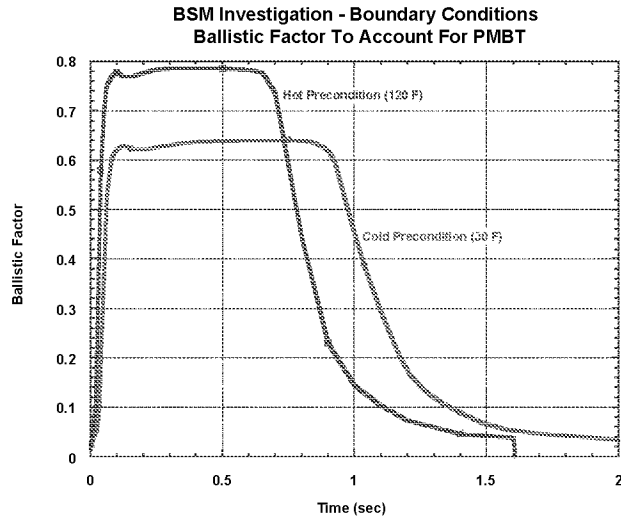


Figure 7: Ballistic Factor

The PATRAN model was translated into SINDA and the environments were applied to the model. The initial temperature of the BSM was assumed to be 120 F. A transient routine was used to generate in-depth thermal response through the throat. A two second simulation was run to investigate the isotherm propagation during soakback as well as during hot-fire. Results were recorded every 0.1 seconds. The data was read back into PATRAN for post-processing and a database of the results was sent to the stress group for structural analysis. The results in Figure 8 represent the results of the thermal analysis at 0.8, 1.2 and 2.0 seconds respectively.

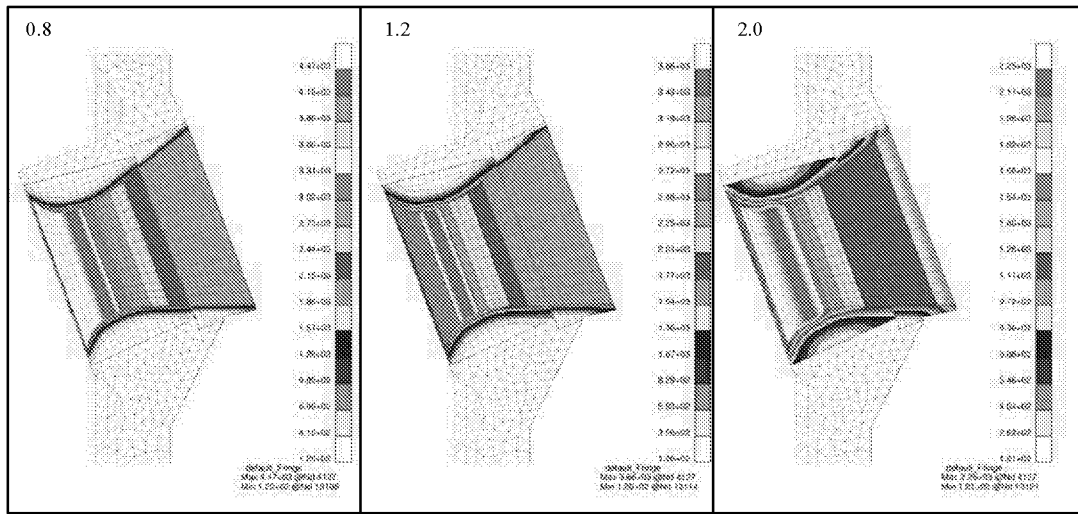


Figure 8: Results From Thermal Model at 0.8, 1.2, and 2.0 seconds. Temperature units are deg F.

Results from the structural analysis did not produce stresses high enough to generate a crack in the throat. Since the material properties of the AJT graphite are well known, the project questioned the accuracy of the thermal model and called upon the thermal community to produce a test that could correlate the model. CSD was able to run some hot-fire test with thermocouples in the adhesive between the graphite throat and the aft housing in an attempt to verify the backside predictions. However, it proved to be extremely difficult to ensure the thermocouple beads would be in contact with the graphite. Since the case is highly pressurized during testing, no holes could be drilled into the case or housing for the thermocouple leads. The only way to get the thermocouples into the gap was to attach them to the backside of the throat prior to assembly. However, during the assembly process, as the throat is slid into the housing, the frictional forces applied to the leads caused the beads to become disconnected from the surface. This made the actual location of the bead hard to verify and since the adhesive has a low conductivity, a thin layer of adhesive between the surface and bead would cause a large gradients to form. Because of this, thermocouple responses were not repeatable. They did, at the very least, indicate that our predictions were in the ballpark, but did not provide data that could be used to correlate the model.

The need to correlate the model still existed, and it appeared that hot-fire testing would not meet the requirements. The data was not conclusive, the boundary conditions could not be verified, testing was depleting valuable assets, and it was expensive. The investigation team began looking for a test facility that could simulate hot-fire test conditions. However, the test requirements were very stringent. To achieve reasonable model correlation, and verification of material properties, the facility had to be able to generate high heat rates very quickly. The stress analysts also wanted to be able to test an entire throat, rather than a sample. This would enable them to correlate hoop stresses and thermal expansion. It was eventually determined that the LHMEEL (Laser Hardened Materials Evaluation Laboratory) facility at Wright-Patterson Air Force Base in Dayton, Ohio, would best fit the test requirements. The LHMEEL facility was established in 1976 as a laboratory to research laser/material interaction of advanced materials for future aerospace systems. LHMEEL 1, a 15-kilowatt continuous wave CO₂ electric discharge coaxial laser (EDCL), was installed at that time. In 1989, LHMEEL II was dedicated. The largest CO₂ laser in the US, LHMEEL II is a 150-kilowatt continuous wave CO₂ EDCL.

SRI (Southern Research Institute) in Birmingham, Alabama, as a subcontractor to CSD, was the organization in charge of designing the tests. Initial flux predictions were still lower than what the throat would experience in a hot-fire test. In an attempt to focus more energy on the throat, SRI contacted Union Carbide, the throat manufacturer, to check the availability of a 2/3-scale throat. Union Carbide provided the scaled throats to SRI for instrumentation. Three tests were designed to generate specific data to be useful in correlating thermal and stress models. The first test was a standard thermal test. It consisted of the 2/3-scale throat bonded into an aluminum housing. Thirteen Type K thermocouples were installed into the fixture by drilling in from the backside. Nine thermocouples were placed on the bondline, while four were placed at known depths within the throat. The second test was known as line-on-line tests. For these tests, the aluminum housing was machined-matched to provide an interference fit with the throat. While these were primarily structural tests, six thermocouples were included. For the third tests, SRI pre-cracked the graphite throat. The purpose of these tests was to determine the ability of the throat to generate debris if it was cracked prior to motor firing, as well as to empirically show the differential heating between the areas above and below the crack. There were eight thermocouples on these tests. Figure 9 shows the fixture for a standard thermal test.

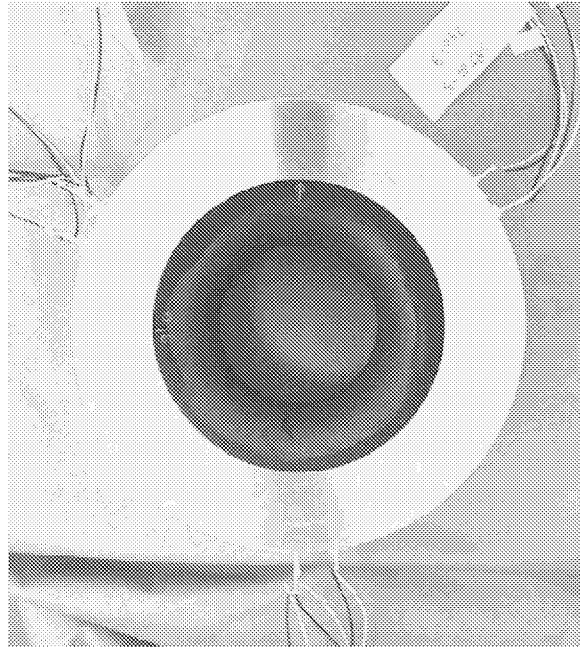


Figure 9: Top View of Standard Thermal Test Set-Up

SRI also designed a mirror to reflect the laser back to the top surface, providing a more uniform flux to the curved throat surface. Figure 10 shows the standard thermal fixture configured for testing. The crimped copper tube on the right side of the picture provided a small airflow above the fixture to remove smoke from the path of the laser. Figure 11 shows the test in process. Notice that the footprint of the laser is slightly elliptical. Also notice the smoke being generated at the top of the throat.

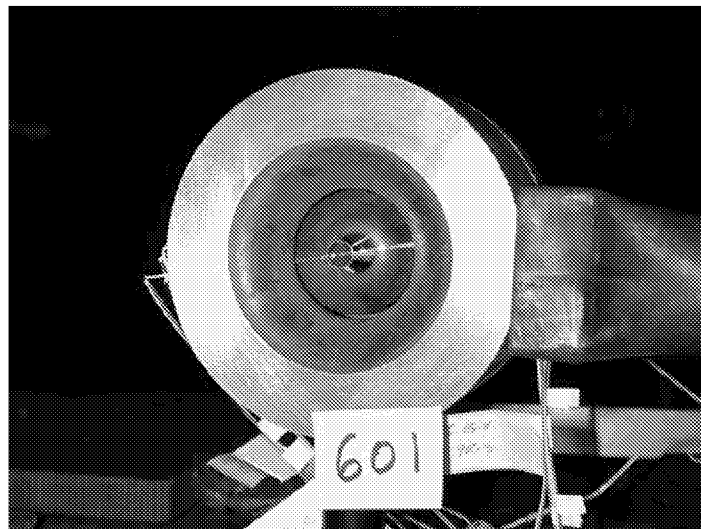


Figure 10: Standard Thermal Fixture Ready For Testing

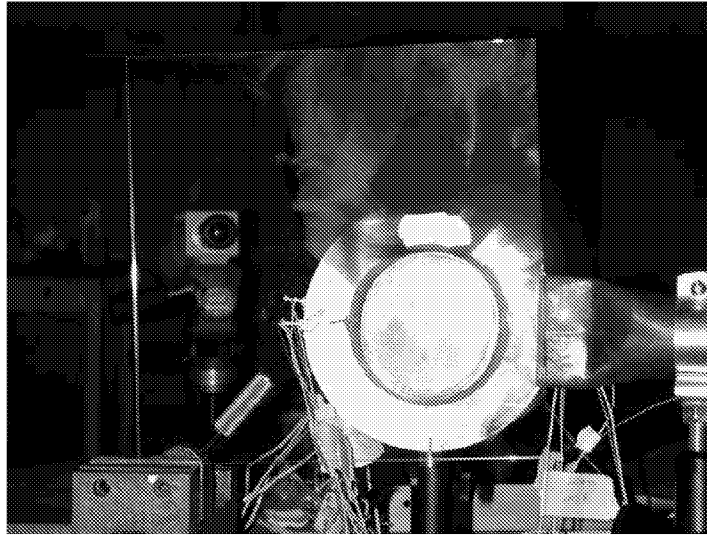


Figure 11: Standard Thermal Fixture During Testing

Since the cross-section of the fixture was constant, and the flux applied to the surface was uniform, a 2-D representation was sufficient. Again, PATRAN was used for pre-processing and interpreted into SINDA. A rendering of the model showing the grid and materials is given in Figure 12.

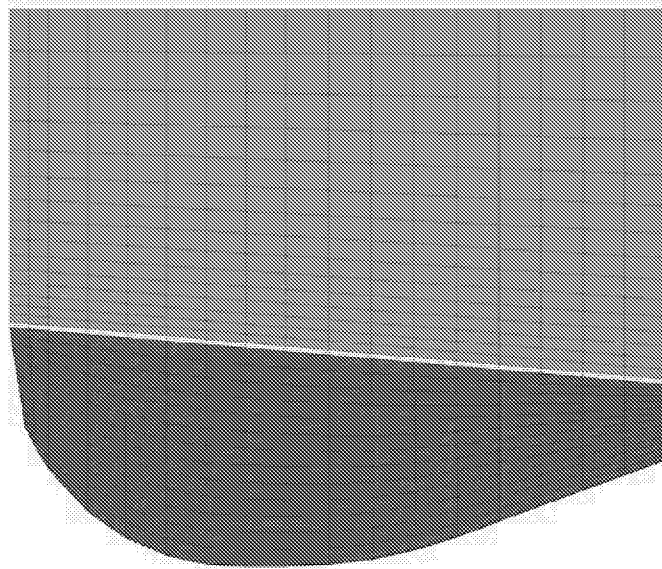


Figure 12: 2-D Model Used To Correlate Standard Thermal Tests

The material properties used for the LHMEI test model were the same properties used in the hot-fire model. The initial temperature was assumed to be the same as the ambient room temperature, 77 F. LHMEI test personnel provide the chart shown in Figure 13. It shows a fairly uniform total flux for all areas above the throat choke-point. In the model, a constant flux of 2100 W/cm² (16.57 BTU/in² sec) was applied to the nodes forward of the choke-point.

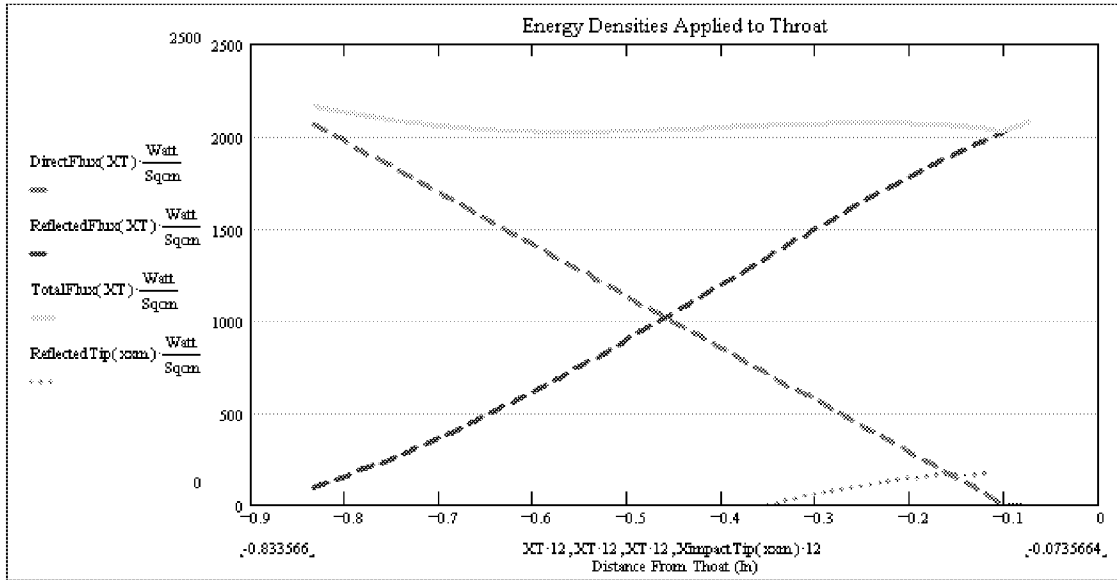


Figure 13: Flux Values From LHMEI Testing

Three one-second standard thermal tests were performed. It had been determined that the thermocouple located 0.500" down from the top surface and 0.200" inside of the bondline should produce the most uniform results. The thermocouple was surrounded by material with homogeneous properties, whereas the bondline thermocouples would likely have more variance in them depending on their location in the epoxy. Each test had a thermocouple 0.500" down and 0.200" inside, at three different radial locations, 60, 180 and 300 degrees. Figure 14 shows the results of the thermal model compared with the all nine thermocouples from the three on-second standard thermal tests.

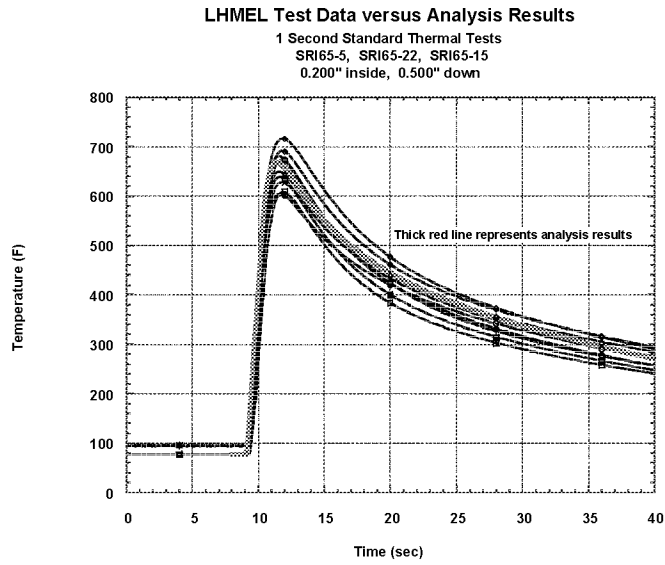


Figure 14: Model Predictions Versus Thermocouple Response For In-Depth Location

Another key correlation location was on the bondline and 0.500" down from the top. Each one second standard thermal test had three thermocouples at this location, clocked radially at 60, 180 and 300 degrees. As was expected, the response of the thermocouples in the bondline had larger variations than thermocouples embedded wholly within the graphite and was less than the model predicted at that location. However, when the predicted temperature of the first layer of epoxy (5 mils back from the back surface of the throat) was plotted along with the thermocouple response, most thermocouples fell with the predicted range. Figure 15 shows these results.

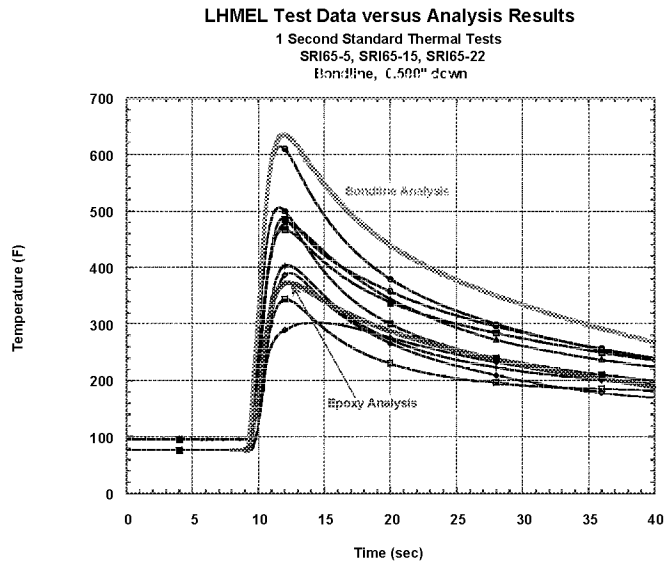


Figure 15: Model Predictions Versus Thermocouple Response For Bondline Location

The LHMEEL tests produced data that was very useful in correlating the original thermal model. The model accurately predicted the test results without any changes to grid fidelity or material properties. Because of this we were able to stand by our original hot-fire predictions. The in-depth response was as good as the initial boundary conditions, which were assumed to be accurate for modeling purposes. Time and financial constraints did not allow for an in-depth testing program to verify combustion environments. However, because of CSD's vast experience with similar motors, and extensive testing and analysis during initial qualification of the BSM's, a high confidence exists in the environments.

Further confirmation of the thermal model came from the second round of LHMEEL testing. Even though the first round was quite successful from a thermal standpoint, it did not produce all of the desired results. Also, there were two throats dedicated to gather thermal expansion data for the stress analyst. For this test, the throat was not contained by an aluminum housing and the only instrumentation were Linear Voltage Differential Transformers (LVDTs). These were called "free-thermal" tests. During this first round of LHMEEL testing, the LVDTs did not work on either test. It was decided to go back to LHMEEL for a second round of testing and do only free-thermal tests. Since this was primarily a structural test, and since there wasn't much time to install thermocouples, the throats were only instrumented with LVDTs. A single thermocouple was taped onto the outer surface simply to act as a monitor. Figure 16 shows the set-up for the free-thermal tests.

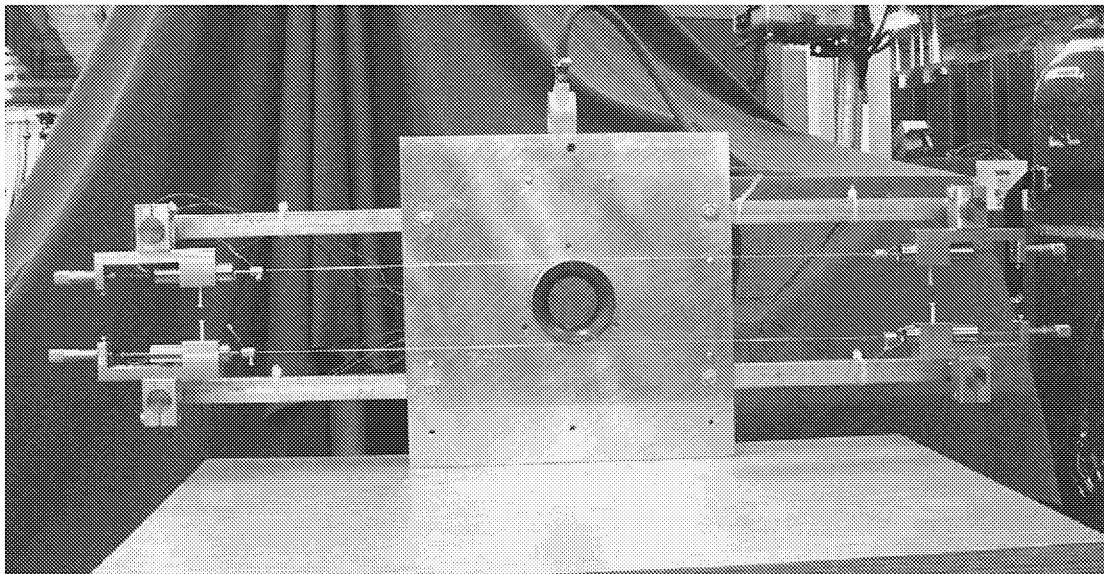


Figure 16: Free Thermal LHMEEL Test Set-Up

For the free-thermal tests, the top backside of the throat had to be machined flat to allow better attachment of the LVDTs. Therefore, a new 2-D grid was developed.

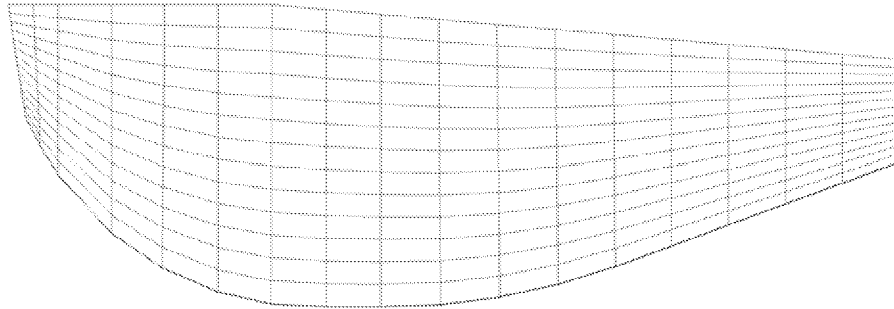


Figure 17: Finite Element Grid for Free-Thermal Tests

The same boundary conditions were applied to the model and the results were sent to stress for input into the structural model. Since there was no appreciable thermal instrumentation on the second round of free thermal tests, verification of the model would come from the results of the combined thermal-structural model. Figure 18 shows the results from that analysis.

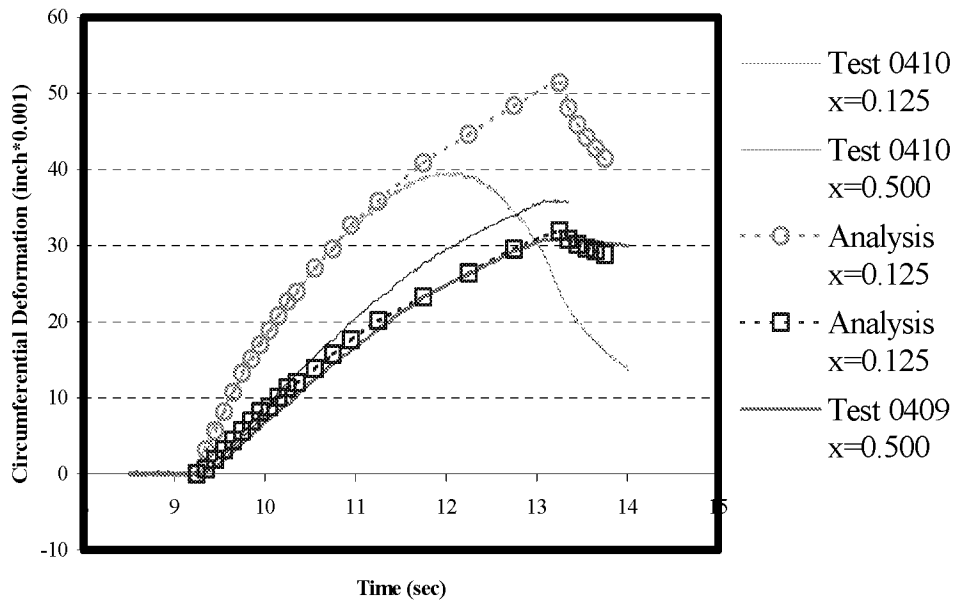


Figure 18: Results From Structural Deformation Model

Since the thermal expansion properties of the AJT graphite are well known, the main variable in the thermal-structural model was the thermal predictions. Since the results of the thermal-structural model matched test results so well, combined with results from the first round of the LHMEI testing indicate that we have high confidence in the model.

The purpose of this paper is to document the process involved in correlating a thermal and combined thermal-structural model. As it was mentioned, there were several LHMEEL tests performed and predictions were made for each test. For brevity, the only data presented here was that which was sufficient to show model correlation. An entire data package was generated showing model-versus-test results. This is currently being submitted as a NASA memorandum and will eventually have a reference number.

The authors would like to acknowledge the contributions of the following people: Eric Poole from NASA/MSFC Strength Analysis Group for the structural analysis, John Koenig and Jacques Cuneo from SRI for excellent support in designing and performing LHMEEL testing, Dave Bidwal from CSD for providing hot-fire boundary conditions and historical material properties, and all of the people at the LHMEEL facility for having a world-class facility and for providing excellent test results.